One-Sided and Two-Sided New Modified EWMA control chart for Detecting Increases in Process Mean

SITTIKORN KHAMROD[1], YUPAPORN AREEPONG[1,*], SAOWANIT SUKPARUNGSEE[1], RAPIN SUNTHORNWAT[2]
[1]Department of Applied Statistics, Faculty of Applied Statistics,
King Mongkut's University of Technology North Bangkok,
Bangkok 10800,
THAILAND

[2]Industrial Technology Program, Faculty of Science and Technology,
Pathumwan Institute of Technology,
Bangkok 10330,
THAILAND

**Corresponding Author*

Abstract: - The main objective of this research is to introduce a new type of control chart, the New Modified EWMA control chart, to detect changes in the process of the average value by studying both one-sided and two-sided control charts. The model studied in this research is the moving average process, or MA(q), with an exponential distribution of residuals. The explicit formula for the average run length of the modified EWMA control chart using the integral equation method to prove the average run lenis are presented. The results of the research found that the average run length obtained has high accuracy and is fast in finding the value when compared to the numerical integral equation method. In this research, several models, such as MA(1), MA(2), and MA(3) processes, were simulated at different parameter levels. In addition, it has been applied to real environmental data, including PM2.5 and PM10 data in Thailand. If the control limits for PM2.5 and PM10 are exceeded, it can be used to identify a potential environmental issue, enabling authorities to investigate the situation and take action before the air quality gets worse.

Key-Words: - exponential white noise, change point detection, Integral equation, new Modified Exponentially Weighted Moving Average, EWMA.

Received: June 13, 2024. Revised: November 9, 2024. Accepted: December 7, 2024. Published: December 31, 2024.

1 Introduction

Quality control aims to evaluate and improve the quality of products and services across various sectors, including finance (especially in trading derivatives and stocks), public health, environmental science, and manufacturing. Statistical process control (SPC) is widely used to identify and address process issues, with control charts being a key tool in this method, [1]. The first control chart introduced by [2] is still widely used to monitor and detect large-scale process changes. Afterward, the exponentially weighted moving average (EWMA) control chart, as introduced by [3] is derived from the Shewhart control chart, which has been shown to be effective in detecting small shifts in the process mean. Furthermore, [4], developed EWMA control charts by adding a constant (k) to the process terms, although in the research of [5] the constant (k) was not defined. The study found that this improved control chart is more effective than the EWMA control chart because it can quickly detect changes in the process average. ARL is a popular measure of control chart performance today, which can be divided into two parts: ARL_0 (Average Run Length when the process is in control) is the average number of points before going out of control. ARL_1 (Average Run Length when the process is out of control) is the average number of points when the process changes until it goes out of control limits, which should be as small as possible. Calculating the ARL involves various methodologies, including Monte Carlo simulation, Markov chains, Martingale techniques, and numerical integration equations (NIE), utilizing different quadrature rules such as midpoint, trapezoidal, Simpson's rule, and Gauss-Legendre [6], [7], [8], [9], [10]. One method involves solving integral equations through explicit formulas. For instance, [11], devised explicit formulas for both ARL and Average Delay Time (ADT) for SMA(1)s on CUSUM charts, while, [12], derived explicit formulas for the ARL of CUSUM control charts for ARIMA(p,d,q) process observations with exponential white noise. [13], proposed an explicit formula for ARL using MA(q) model observations, assessing its ability to detect minor changes in data autocorrelated with white noise.

The study, [14], also defines an explicit formulation for the ARL of the MAX(1,1) model. A new modified EWMA control chart, designed to detect small changes in the process means better than the EWMA chart, demonstrates increased sensitivity, enabling the rapid detection of small changes. This capability is crucial for maintaining product quality and reducing process variation. These methodologies can be effectively applied to precise data.

Currently, many countries are facing problems related to air pollution, which can be measured by PM2.5 and PM10 values. PM2.5 and PM10 refer to particles with a diameter of 2.5 and 10 micrometers or less, respectively. These particles originate from natural sources such as soil and seawater, as well as human activities such as fossil fuel combustion, industrial processes, and vehicle exhaust emissions. PM2.5 particles are smaller and therefore more harmful to human health because they can penetrate deep into the lungs and bloodstream, resulting in health problems such as respiratory and cardiovascular diseases, [15], [16]. Previous studies on the performance of control charts indicate that the average run length (ARL) can be used to compare the performance of charts. Therefore, this research aims to compare the performance of standard EWMA, modified EWMA, and a new modified EWMA control charts to detect small changes by considering the ARL values. In this research, these control charts are also applied to detect changes in PM2.5 and PM10 levels in Thailand by collecting daily data from the National Research Council of Thailand (NRCT) from June 27, 2022, to April 6, 2023.

2 The Characteristics of the Diverse EWMA Control Chart

2.1 The EWMA Control Chart

By applying the recursive equation, one can derive the EWMA control chart, a tool designed to monitor and detect subtle changes in the process mean, as described by [2].

$$E_t = (1-\lambda)E_{t-1} + \lambda Y_t\,,\ t = 1, 2, 3, \ldots \tag{1}$$

where E_t is the EWMA statistic, where λ is an exponential smoothing parameter $(0 < \lambda < 1)$, and Y_t is the sequence of the MA(q) process with exponential white noise. Thus, the general upper control limit (*UCL*) and lower control limit (*LCL*) for detecting the sequence are given as follows:

$$UCL = \mu_0 + L_1\sigma\sqrt{\frac{\lambda}{2-\lambda}} \tag{2}$$

$$LCL = \mu_0 - L_1\sigma\sqrt{\frac{\lambda}{2-\lambda}} \tag{3}$$

where μ_0 is the target mean, σ is the process standard deviation, and L_1 is an appropriate control width limit $(L_1 > 0)$. The *UCL* and *LCL* mean and variance of the EWMA control chart are $E(E_t) = \mu_0$ and $\mathrm{Var}(E_t) = \sigma^2(\frac{\lambda}{2-\lambda}),$ respectively.

The stopping time for the one-sided EWMA control chart is determined by:

$$\zeta_h = \{t > 0 : E_t < g \text{ and } E_t > h\} \tag{4}$$

2.2 The Modified EWMA Control Chart

[4], introduced a novel configuration for the control statistics of the modified EWMA control chart, utilizing the provided recursive equation.

$$Z_t = (1-\lambda)Z_{t-1} + \lambda Y_t + k(Y_t - Y_{t-1}) \tag{5}$$

where λ is an exponential smoothing parameter $(0 < \lambda < 1)$ and k is a constant $(k > 0)$. The mean and variance of the modified EWMA control chart are $E(Z_t) = \mu_0$ and $\mathrm{Var}(Z_t) = \sigma^2(\frac{\lambda + 2\lambda k + 2k^2}{2-\lambda}),$

respectively. Consequently, the general *UCL* and *LCL* to detect the sequence are given as follows:

$$UCL = \mu_0 + L_2\sigma\sqrt{\frac{\lambda + 2\lambda k + 2k^2}{2-\lambda}} \tag{6}$$

$$LCL = \mu_0 - L_2\sigma\sqrt{\frac{\lambda + 2\lambda k + 2k^2}{2-\lambda}} \tag{7}$$

where μ_0 is the target mean, σ is the process standard deviation, L_2 is an appropriate control width limit $(L_2 > 0)$, Y_t is the sequence of the MA(q) process with exponential white noise, $Z_0 = u$ and $Y_0 = v$ are the initial values, and $0 < \lambda \le 1$ is an exponential smoothing parameter.
The stopping time for the one-sided modified EWMA control chart is determined by:

$$\zeta_b = \{t > 0 : Z_t < a \text{ and } Z_t > b\} \tag{8}$$

where ζ_b is the stopping time, a is the *LCL*, and b is the *UCL*.

2.3 The New Modified EWMA Control Chart

Expanding upon the model proposed by [4], the latest version of the modified EWMA control chart has been enhanced by introducing an additional constant into the equation. These extra constant underscores the significance of current data over historical data. The formulation of the new modified EWMA control chart incorporates three constants: k, k_1, and k_2. In the original EWMA control chart, [3], set $k_1 = k_2 = 1$, while, [4], suggested a modification with $k_1 = k_2$, and, [5] further refined it with $k_1 = k_2 = 1$. The structure of the new modified EWMA control chart is delineated as follows:

$$M_t = (1-\lambda)M_{t-1} + \lambda Y_t + k_1 Y_t - k_2 Y_{t-1} \tag{9}$$

where λ is an exponential smoothing parameter $(0 < \lambda < 1)$ and k_1 and k_2 are constants $(k_1 > k_2 > 0)$. The mean and variance of the new modified EWMA control chart are $E(M_t) = (\lambda + k_1 - k_2)\frac{\mu_0}{\lambda}$ and $\mathrm{Var}(M_t)$ $= \sigma^2\left(\frac{(\lambda+k_1)^2 + k_2^2 - 2\lambda k_2 + 2\lambda^2 k_2 - 2k_1k_2 + 2\lambda k_1 k_2}{\lambda(2-\lambda)}\right)$ respectively.

Consequently, the general UCL and LCL to detect the sequence are given as follows:

$$UCL = (\lambda + k_1 - k_2)\frac{\mu_0}{\lambda} + L_3\sigma\sqrt{\frac{(\lambda+k_1)^2 + k_2^2 - 2\lambda k_2 + 2\lambda^2 k_2 - 2k_1k_2 + 2\lambda k_1 k_2}{\lambda(2-\lambda)}} \tag{10}$$

$$LCL = (\lambda + k_1 - k_2)\frac{\mu_0}{\lambda} - L_3\sigma\sqrt{\frac{(\lambda+k_1)^2 + k_2^2 - 2\lambda k_2 + 2\lambda^2 k_2 - 2k_1k_2 + 2\lambda k_1 k_2}{\lambda(2-\lambda)}} \tag{11}$$

The stopping time for the one-sided new modified EWMA control chart is determined by

$$\psi_b = \{t > 0 : M_t < l \text{ and } M_t > f\}$$

where L_3 is an appropriate control width limit $(L_3 > 0)$.

3 The ARL of New Modified EWMA Control Chart

3.1 The Exact Solution of ARL the New Modified EWMA Control Chart for MA(q) Process with Exponential White Noise

A process of deriving a MA(q) with exponential white noise can be accomplished by:

$$Y_t = \mu + \varepsilon_t - \theta_1\varepsilon_{t-1} - \theta_2\varepsilon_{t-2} - \ldots - \theta_q\varepsilon_{t-q}; \quad t = 1,2,3,\ldots \tag{12}$$

where μ is a constant, ε_t is the white noise process $\varepsilon_t \sim Exp(\alpha)$, θ is the MA(q) coefficient with an initial value of $\varepsilon_0 = s$. Consequently, the new modified EWMA statistic (M_t) can be formulated as:

$$M_t = (1-\lambda)M_{t-1} + (\lambda + k_1)(\mu - \theta_1\varepsilon_{t-1} - \ldots - \theta_q\varepsilon_{t-q}) + (\lambda + k_1)\varepsilon_t - k_2 Y_{t-1}.$$

If Y_1 signals the out-of-control state for M_1 when $M_0 = u$, then

$$M_1 = (1-\lambda)u + (\lambda + k_1)(\mu - \theta_1\varepsilon_{t-1} - \ldots - \theta_q\varepsilon_{t-q}) + (\lambda + k_1)\varepsilon_1 - k_2 Y_{t-1}.$$

If ε_1 is the in-control limit for M_1, then $l \le M_1 \le f$.
Consider the following function:

$$F(u) = 1 + \int F(M_1) f(\varepsilon_1) d(\varepsilon_1) \tag{13}$$

which is a Fredholm integral equation of the second kind. Moreover, $F(u)$ can be rewritten as

$$F\left(u\right)=1+\int_{l}^{f}F(\left(1-\lambda\right)u+\left(\lambda+k_1\right)(\mu-\theta_1\varepsilon_{t-1}-\ldots -\theta_q\varepsilon_{t-q})-k_2Y_{t-1}+\left(\lambda+k_1\right)y)f\left(y\right)dy \tag{14}$$

Let $w=\left(1-\lambda\right)u-k_2Y_{t-1}+\left(\lambda+k_1\right)y +\left(\lambda+k_1\right)(\mu-\theta_1\varepsilon_{t-1}-\ldots-\theta_q\varepsilon_{t-q})$.

By adjusting the integral variable, we derive the subsequent integral equation:

$$F\left(u\right)=1+\frac{1}{\lambda+k_1}\int_{l}^{f}F\left(w\right)f(\frac{w-\left(1-\lambda\right)u}{\left(\lambda+k_1\right)}+\frac{k_2Y_{t-1}}{\left(\lambda+k_1\right)} -\mu+\theta_1\varepsilon_{t-1}+\ldots+\theta_q\varepsilon_{t-q})dw \tag{15}$$

If $Y_t \sim Exp\left(\alpha\right)$ the $f\left(y\right)=\frac{1}{\alpha}e^{\frac{-y}{\alpha}}$; $y\geq 0$, then

$$F\left(u\right)=1+\frac{1}{\lambda+k_1}\int_{l}^{f}F\left(w\right)\frac{1}{\alpha}e^{\frac{-w}{\alpha\left(\lambda+k_1\right)}} \times e^{\frac{(1-\lambda)u-k_2Y_{t-1}}{\alpha(\lambda+k_1)}+\frac{1}{\alpha}\left\{\mu-\theta_1\varepsilon_{t-1}-\ldots-\theta_q\varepsilon_{t-q}\right\}}dw. \tag{16}$$

Let function $C\left(u\right)=e^{\frac{(1-\lambda)u-k_2Y_{t-1}}{\alpha(\lambda+k_1)}+\frac{1}{\alpha}\left\{\mu-\theta_1\varepsilon_{t-1}-\ldots-\theta_q\varepsilon_{t-q}\right\}}$, then we have

$$F\left(u\right)=1+\frac{C\left(u\right)}{\alpha\left(\lambda+k_1\right)}\int_{l}^{f}F\left(w\right)e^{\frac{-w}{\alpha(\lambda+k_1)}}dw \;;\; l\leq u\leq f .$$

Let $g=\int_{l}^{f}F\left(w\right)e^{\frac{-w}{\alpha(\lambda+k_1)}}dw$, then $F\left(u\right)=1+\frac{C\left(u\right)}{\alpha\left(\lambda+k_1\right)}\cdot g.$.

Consequently, we obtain

$$F(u)=1+\frac{1}{\alpha\left(\lambda+k_1\right)}e^{\frac{(1-\lambda)u-k_2Y_{t-1}}{\alpha(\lambda+k_1)}+\frac{\mu}{\alpha}+\frac{-\theta_1\varepsilon_{t-1}-\ldots-\theta_q\varepsilon_{t-q}}{\alpha}}\cdot g . \tag{17}$$

By solving for constant g, we obtain

$$\begin{aligned}
g &=\int_{l}^{f}F\left(w\right)e^{\frac{-w}{\alpha(\lambda+k_1)}}dw \\
&=\int_{l}^{f}\left[1+\frac{B}{\alpha\left(\lambda+k_1\right)}C\left(w\right)\right]e^{\frac{-w}{\alpha(\lambda+k_1)}}dw \\
&=\int_{l}^{f}e^{\frac{-w}{\alpha(\lambda+k_1)}}dw+\int_{l}^{f}\frac{ge^{\frac{(1-\lambda)w-k_2Y_{t-1}}{\alpha(\lambda+k_1)}+\frac{1}{\alpha}\left\{\mu-\theta_1\varepsilon_{t-1}-\ldots-\theta_q\varepsilon_{t-q}\right\}}}{\alpha\left(\lambda+k_1\right)} \times e^{\frac{-w}{\alpha(\lambda+k_1)}}dw
\end{aligned}$$

$$g=\frac{-\alpha\left(\lambda+k_1\right)(e^{\frac{-f}{\alpha(\lambda+k_1)}}-e^{\frac{-l}{\alpha(\lambda+k_1)}})}{1+\frac{e^{-\frac{k_2Y_{t-1}}{\alpha(\lambda+k_1)}+\frac{1}{\alpha}\left\{\mu-\theta_1\varepsilon_{t-1}-\ldots-\theta_q\varepsilon_{t-q}\right\}}}{\lambda}\times(e^{\frac{-\lambda f}{\alpha(\lambda+k_1)}}-e^{\frac{-\lambda l}{\alpha(\lambda+k_1)}})} . \tag{18}$$

Substituting the constant g into Equation (17) leads us to:

$$F(u)=1+\frac{e^{\left\{\frac{(1-\lambda)u}{\alpha(\lambda+k_1)}-\frac{k_2Y_{t-1}}{\alpha(\lambda+k_1)}+\frac{1}{\alpha}(\mu-\theta_1\varepsilon_{t-1}-\ldots-\theta_q\varepsilon_{t-q})\right\}}}{\alpha\left(\lambda+k_1\right)} \times(\frac{-\alpha\left(\lambda+k_1\right)(e^{\frac{-f}{\alpha(\lambda+k_1)}}-e^{\frac{-l}{\alpha(\lambda+k_1)}})}{1+\frac{e^{\left\{-\frac{k_2Y_{t-1}}{\alpha(\lambda+k_1)}+\frac{1}{\alpha}(\mu-\theta_1\varepsilon_{t-1}-\ldots-\theta_q\varepsilon_{t-q})\right\}}}{\lambda}(e^{\frac{-\lambda f}{\alpha(\lambda+k_1)}}-e^{\frac{-\lambda l}{\alpha(\lambda+k_1)}})}) . \tag{19}$$

Consequently, by utilizing the Fredholm integral equation of the second kind, we can delineate the exact two-sided formulas for the ARL of an MA(q) process operating on the new modified EWMA control chart as follows:

$$ARL_{2-sided}=1-\frac{\lambda e^{\frac{(1-\lambda)u}{\alpha(\lambda+k_1)}}(e^{\frac{-f}{\alpha(\lambda+k_1)}}-e^{\frac{-l}{\alpha(\lambda+k_1)}})}{\lambda e^{\frac{k_2Y_{t-1}}{\alpha(\lambda+k_1)}-\frac{1}{\alpha}(\mu-\theta_1\varepsilon_{t-1}-\ldots-\theta_q\varepsilon_{t-q})}+e^{\frac{-\lambda f}{\alpha(\lambda+k_1)}}-e^{\frac{-\lambda l}{\alpha(\lambda+k_1)}}} . \tag{20}$$

In the scenario where $l = 0$, the explicit one-sided formulas for the ARL of an MA(q) process implemented on the new modified EWMA control chart can be depicted as follows:

$$ARL_{1-sided}=1-\frac{\lambda e^{\frac{(1-\lambda)u}{\alpha(\lambda+k_1)}}\left[e^{\frac{-f}{\alpha(\lambda+k_1)}}-1\right]}{\lambda e^{\frac{k_2Y_{t-1}}{\alpha(\lambda+k_1)}-\frac{1}{\alpha}(\mu-\theta_1\varepsilon_{t-1}-\ldots-\theta_q\varepsilon_{t-q})}+e^{\frac{-\lambda f}{\alpha(\lambda+k_1)}}-1} \tag{21}$$

3.2 The Existence and Uniqueness of the Explicit Formulas

We show the existence and uniqueness of the solution to the integral equation in Eq.(16) define by:

$$T\left(F\left(u\right)\right)=1+\frac{1}{\lambda+k_1}\int_{l}^{f}F\left(w\right) \times\frac{1}{\alpha}e^{-\frac{1}{\alpha}\left\{\frac{w-(1-\lambda)u}{(\lambda+k_1)}+\frac{k_2Y_{t-1}}{(\lambda+k_1)}-\mu+\theta_1\varepsilon_{t-1}+\ldots+\theta_q\varepsilon_{t-q}\right\}}dw \tag{22}$$

Theorem 1. Banach's fixed-point theorem, [17].

Let $M[l,f]$ represent the set comprising all continuous functions on complete metric space (X,d), and let $T:X\to X$ represent a contraction mapping with a contraction constant $0\le g<1$; i.e., $\|T(F_1)-T(F_2)\| \le g\|F_1-F_2\| \ \forall F_1,F_2\in X$. Subsequently, $F(.)\in X$ is unique at $T(F(u)) = F(u)$; i.e., there exists only one fixed point within the set X.

Proof: To demonstrate that T, as defined in Eq. (16), acts as a contraction mapping for $F_1,F_2\in C[l,f]$, we employ the inequality $\|T(F_1)-T(F_2)\|\le s\|F_1-F_2\| \ \forall F_1$, $F_2\in C[l,f]$ with $0\le s<1$. Regard Eq.(8) and Eq.(16), then

$$\|T(F_1)-T(F_2)\|_\infty$$

$$=\sup_{u\in[l,f]}\left|\frac{C(u)}{\alpha(\lambda+k)}\int_l^f (F_1(w)-F_2(w))e^{\frac{-w}{\alpha(\lambda+k)}}dw\right|$$

$$\le\sup_{u\in[l,f]}\left|\|F_1-F_2\|_\infty C(u)\left(e^{\frac{-l}{\alpha(\lambda+k_1)}}-e^{\frac{-f}{\alpha(\lambda+k_1)}}\right)\right|$$

$$=\|F_1-F_2\|_\infty\left|1-e^{\frac{-l}{\alpha(\lambda+k)}}\right|\sup_{u\in[l,h]}|C(u)|$$

$$\le s\|F_1-F_2\|_\infty,$$

where $s=\left|e^{\frac{-l}{\alpha(\lambda+k_1)}}-e^{\frac{-f}{\alpha(\lambda+k_1)}}\right|\sup_{u\in[l,f]}|C(u)|$ and

$$C(u)=e^{\frac{(1-\lambda)u-k_2Y_{t-1}}{\alpha(\lambda+k_1)}+\frac{1}{\alpha}\{\mu-\theta_1\varepsilon_{t-1}-\dots-\theta_q\varepsilon_{t-q}\}};0\le s<1.$$

By applying Banach's fixed-point theorem, we establish that the solution exists uniquely.

3.3 Numerical Integral Equation of ARL for MA(q) Process

The Numerical Integral Equation (NIE) method is a computational technique employed to calculate the Average Run Length (ARL) for a Moving Average process of order q, referred to as MA(q). The ARL is an essential measure in statistical process control, representing the anticipated number of observations before an out-of-control signal is detected. Calculating the ARL for an MA(q) process with exponential white noise is complex due to the autocorrelation present in the process data.

In ARL assessment, the NIE method is extensively used and can be implemented with various quadrature rules such as midpoint, trapezoidal, Simpson's rule, and Gauss-Legendre, all of which yield ARL values that are highly similar. This study employs the Gauss-Legendre rule to compute the ARL. Through the integral equation, a second-order approximation for the ARL on the new modified EWMA control chart for the MA(q) process in Eq.(19) can be derived. Utilizing the Gauss-Legendre quadrature rule is fundamental to this process.

$$f(a_j)=f(\frac{a_j-(1-\lambda)a_i}{(\lambda+k_1)}+\frac{k_2Y_{t-1}}{(\lambda+k_1)}-\mu+\theta_1\varepsilon_{t-1}+\dots+\theta_q\varepsilon_{t-q}). \quad (23)$$

The representation of an integral approximation can be expressed as:

$$\int_l^f F(w)f(w)dw\approx\sum_{j=1}^m w_jf(a_j) \quad (24)$$

where $a_j=\frac{f-l}{m}\left(j-\frac{1}{2}\right)+l$ and

$$w_j=\frac{f-l}{m};j=1,2,...,m.$$

The Gauss-Legendre quadrature rule enables the approximation of the integral equation as depicted below:

$$\tilde{F}(a_i)=1+\frac{1}{\lambda+k_1}\sum_{j=1}^m w_j\tilde{F}(a_j)f(\frac{a_j-(1-\lambda)a_i}{(\lambda+k_1)}+\frac{k_2Y_{t-1}}{(\lambda+k_1)}-\mu+\theta_1\varepsilon_{t-1}+\dots+\theta_q\varepsilon_{t-q}) \quad (25)$$

3.4 Performance Evaluation

In this analysis, we compare the findings for ARL_0 and ARL_1, calculated using explicit formulas and the NIE method, for a MA(q) process with exponential white noise running on a new modified EWMA chart. The numerical results were computed using MATHEMATICA, with a division point of 1,000. The accuracy of the ARL values is compared with the percentage accuracy which can be obtained from

$$\%ACC=100-\left|\frac{k(v)-\tilde{k}(v)}{k(v)}\right|\times100\%. \quad (26)$$

where $k(v)$ is ARLs of the explicit formulas values, and $\tilde{k}(v)$ is ARLs of the NIE method values.

In performance assessment is conducted with the average extra quadratic loss (*AEQL*), derived as:

$$AEQL = \frac{1}{\delta_{\max}} \sum_{0}^{\delta_{\max}} \delta^2 \times ARL(\delta) \,. \tag{27}$$

The parameter δ is defined within the range $0 < \delta < \delta_{\max}$, where $\delta_{\max}$ represents the largest location process shift under examination. A smaller value of the *AEQL* indicates a higher proficiency of the chart in detecting the location process shift. Moreover, the relative mean index (*RMI*) is utilized as the performance indicator to evaluate the ARL of a MA(q) process with exponential white noise on both the EWMA and new modified EWMA control charts.

$$RMI = \frac{1}{n} \sum_{i=1}^{n} \left(\frac{ARL_{shift,i} - Min[ARL_{shift,i}]}{Min[ARL_{shift,i}]} \right) \tag{28}$$

where $ARL_{shift,i}$ is the ARL of the control chart when a shift in the process mean is detected and $Min[ARL_{shift,i}]$ is the minimum value of the ARL at the same level.

4 Numerical Results

This section presented the ARL results of a MA(q) process with exponential white noise on the new modified EWMA control chart in Table 1 (Appendix) and Table 2 (Appendix). Table 1 displayed findings for different θ values with $\mu = 2$, k_1=2, and k_2=1.5 for the MA(1) process, while Table 2 showed results for varied θ_3 values with $\mu = 2$, $\theta_1 = 0.1, \theta_2 = 0.2$, k_1=3, and k_2=2.5 for the MA(3) process CPU time (System: AMD Ryzen 7 5700U with Radeon Graphics@1.8GHz. Processor, 16GB RAM. 64-bit Operating System) for both explicit formulas and the NIE method was included in these tables. Furthermore, Table 3 (Appendix) provided a performance assessment of the one-sided ARL for the MA(2) process across EWMA, modified, and new modified EWMA control charts, considering parameters such as ARL_0 = 370, λ = 0.05, 0.10, and 0.20, $\mu = 1.5$, $\theta_1 = 0.1, \theta_2 = 0.2$, shift sizes of 0.001, 0.003, 0.005, 0.01, 0.03, 0.05, 0.10, 0.30, 0.50, and 1.00. Table 4 (Appendix) offered a two-sided comparison of ARL for the MA(3) process on EWMA, modified, and new modified EWMA control charts, with parameters including ARL_0 = 370, λ = 0.05, 0.10, and 0.20, $\mu = 1$, $\theta_1 = 0.1, \theta_2 = 0.2, \theta_3 =$ 0.3, shift sizes of 0.001, 0.003, 0.005, 0.01, 0.03, 0.05, 0.10, 0.30, 0.50, and 1.00.

Results from Tables 1 and 2 indicated that ARL values obtained through explicit formulas were identical to those derived from the NIE method, affirming a numerical accuracy of 100%. Notably, the computational time for explicit formulas was significantly shorter, taking less than 1 second, whereas the NIE method required around 10 seconds. Tables 3 and 4 showcased consistently smaller ARL values for the newly modified EWMA control chart computed through explicit formulas compared to the EWMA and modified EWMA control charts across most conditions, except for specific cases such as λ = 0.05 and shift sizes of 0.05 and 1.00. Furthermore, RMI and AEQL values for ARL on the newly modified EWMA control chart were lower than those for the EWMA and modified EWMA control charts. Findings also indicated that decreasing k_1 led to increased ARL values, while decreasing k_2 and increasing shift size resulted in decreased ARL values. The new modified EWMA control chart demonstrates a quicker detection of out-of-control conditions (smaller ARL values), enhanced numerical accuracy, reduced RMI and AEQL values, and strong sensitivity to parameter variations, reflecting its superior capability in minimizing false alarms and efficiently identifying process shifts. Finally, Figure 1 provides a succinct overview of the simulation outcomes.

Applications*: *Daily data of PM2.5 and PM10

This section provides a synthesis of the daily PM2.5 and PM10 data from June 27, 2022, to April 6, 2023, summarized in Tables 5 and 6. The performance of the new modified EWMA control chart outperformed both the EWMA and modified EWMA control charts across all parameter settings, as indicated by the smallest *RMI* and *AEQL* values observed with the new modified EWMA control chart. Moreover, reducing the value of k_2 resulted in a decline in ARL values. Additionally, ARL values decreased with an increase in shift size, as depicted in Figures 3 and 4, respectively. Within this part, Figure 2 illustrates the ARL values for example 1, demonstrating coherence with the findings derived from simulations. These results underscore the enhanced efficiency of the new modified EWMA control chart in comparison to alternative methods.

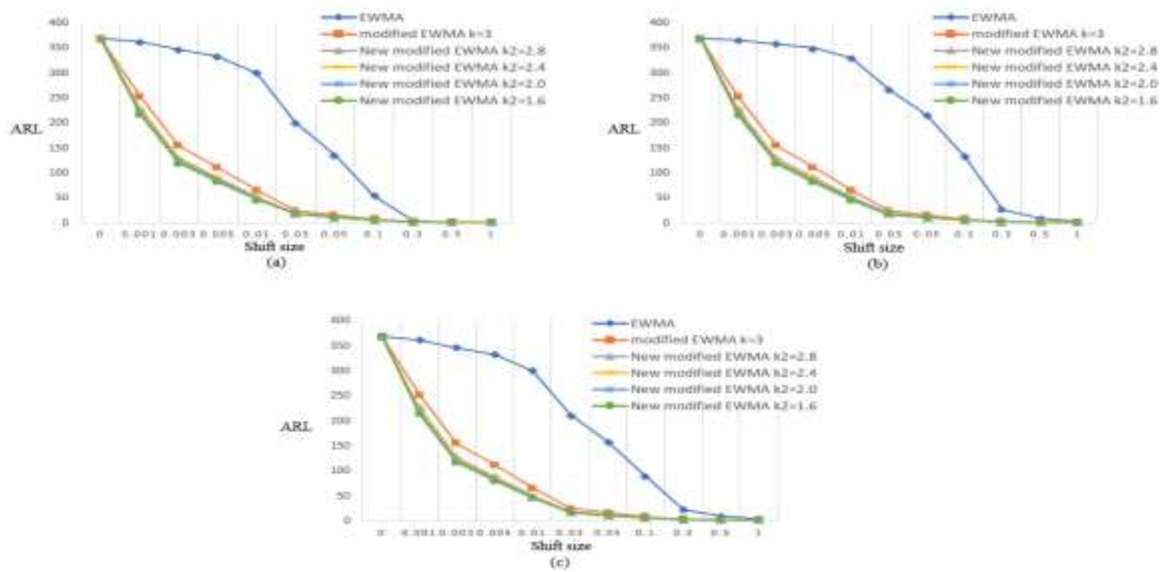

Fig. 1: The ARL of the EWMA, modified EWMA, and new modified EWMA control charts simulation data for (a) $\lambda = 0.05$, (b), $\lambda = 0.10$ and (c) $\lambda = 0.20$

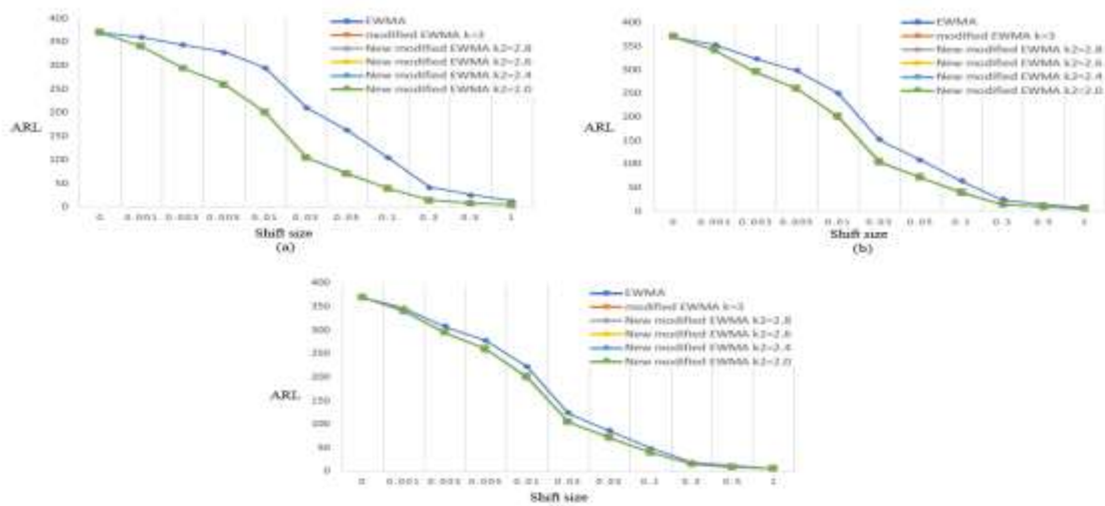

Fig. 2: The ARL of the EWMA, modified EWMA, and new modified EWMA control charts for example 1 when (a) $\lambda = 0.05$, (b), $\lambda = 0.10$ and (c) $\lambda = 0.20$

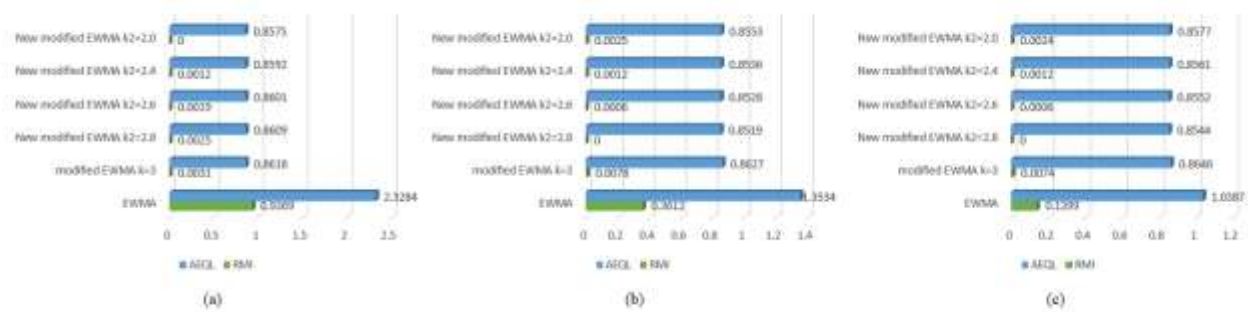

Fig. 3: The AEQL and RMI values of the EWMA, modified EWMA, and new modified EWMA control charts for example 1 when (a) $\lambda = 0.05$, (b), $\lambda = 0.10$ and (c) $\lambda = 0.20$

Fig. 4: The AEQL and RMI values of the EWMA, modified EWMA, and new modified EWMA control charts for example 2 when (a) $\lambda = 0.05$, (b), $\lambda = 0.10$ and (c) $\lambda = 0.20$

5 Conclusion

The explicit formulas were derived to determine the ARL of a MA(q) process with exponential white noise on the new modified EWMA control chart and were compared in accuracy with the NIE method using percentage accuracy values. Results revealed comparable performance between both methods, achieving 100% accuracy. Notably, the explicit formulas demonstrated significantly faster computation times, with CPU times of less than 1 second. Comparative analysis of ARL derived from explicit formulas across EWMA, modified EWMA, and new modified EWMA control charts showed the latter to be more proficient in detecting changes than the former two, utilizing criteria such as the RMI and AEQL. Real-world PM2.5 and PM10 data were utilized to evaluate the effectiveness of the proposed control chart, with analysis results mirroring simulation outcomes. Overall, the findings indicate that explicit formulas for ARL of a MA(q) process with exponential white noise enable quicker detection of process changes mean on the new modified EWMA control chart compared to EWMA and modified EWMA control charts. Moreover, extending the application of the New Modified EWMA control chart to other pollutants and industries, combined with the development of enhanced algorithms, provides a comprehensive solution for future research. This integrated approach will validate, expand, and solidify the applicability of the New Modified EWMA control chart as a crucial tool in modern quality control practices.

Acknowledgement:

This research was funded by Thailand Science Research and Innovation Fund (NSRF), and King Mongkut's University of Technology North Bangkok with Contract no. KMUTNB-FF-67-B-12.

Declaration of Generative AI and AI-assisted technologies in the writing process

During the preparation of this work the authors used QuillBot in order to modify a few phrases in abstract and introduction sections to enhance academic quality. After using this tool/service, the authors reviewed and edited the content as needed and take(s) full responsibility for the content of the publication.

References:

[1] M. Kovarik, P. Klimek, The usage of time series control charts for financial process analysis. *Journal of Competitiveness*. Vol. 4, No.3, 2012, pp.29-45. https://doi.org/10.7441/joc.2012.03.03.

[2] W. A. Shewhart. Economic control of quality of manufactured product, D. Van Nostrand Company, New York, NY, 1931, https://doi.org/10.2307/2301530

[3] S. W. Roberts, Control chart tests based on geometric moving average, *Technometrics*, Vol 1, No. 3, 1959, pp. 239-250. https://doi.org/10.1080/00401706.2000.10485986.

[4] N. Khan, M. Aslam, C-H. Jun. Design of a control chart using a modified EWMA statistic. *Quality and Reliability Engineering International*. Vol.33, 2017, pp.1095–1104. https://doi.org/10.1002/qre.2102.

[5] A. K. Patel, J. Divecha. Modified exponentially weighted moving average (EWMA) control chart for an analytical process data. *Journal of Chemical Engineering and Materials Science*, Vol.2, No.1, 2011, pp.12-20, [Online]. https://academicjournals.org/journal/JCEMS/article-full-text-pdf/466796E1469 (Accessed Date: September 10, 2024.

[6] V. Alevizakos, K. Chatterjee, C. Koukouvinos. Modified EWMA and DEWMA control charts for process monitoring. *Communications in Statistics-Theory and Methods*, Vol.51, No.21, 2022, pp.7390-7412. https://doi.org/10.1080/03610926.2021.1872642.

[7] S. Phanyaem, Explicit formulas and numerical integral equation of ARL for SARX (P, r) L model based on CUSUM chart. *Mathematics and Statistics*, Vol.10, No.1, 2022, pp. 88-99. DOI: 10.13189/ms.2022.100107.

[8] W. Suriyakat, K. Petcharat, Exact run length computation on EWMA control chart for stationary moving average process with exogenous variables. *Mathematics and Statistics*, Vol.10, No.3, 2022, pp. 624-635. DOI: 10.13189/ms.2022.100319.

[9] K. Petcharat, Designing the performance of EWMA control chart for seasonal moving average process with exogenous variables. *IAENG International Journal of Applied Mathematics*, Vol.53, No.2, 2023, pp. 757-765.

[10] Ratmila, E. T HerdianiErna, S. Sunusi, A Modified Exponentially Weighted Moving Average for Monitoring Zero Inflated Generalized Poisson Processes. *International Journal of Research Publications (IJRP)*, Vol.134, No.1, 2023, pp.103-114. https://doi.org/10.47119/IJRP100134110202355537.

[11] P. Busababodin, An analytical of ARL for seasonal $MA(1)_S$ on CUSUM chart. In *Proceeding of International Conference on Applied Statistics*, *Khon Kean, Thailand*, 2014, pp. 176 – 182.

[12] L. Zhang, P. Busababodhin, The ARIMA (p, d, q) on Upper Sided of CUSUM Procedure. *Lobachevskii Journal of Mathematics*, Vol.39, 2018, pp. 424 – 432. https://doi.org/https://doi.org/10.1134/S1995080218030216.

[13] Y. Supharakonsakun, Statistical design for monitoring process mean of a modified EWMA control chart based on autocorrelated data. *Walailak Journal of Science and Technology (WJST)*, Vol.18, No.12, 2021, pp. 19813-12. https://doi.org/10.48048/wjst.2021.19813.

[14] S. Khamrod, Y. Areepong, S. Sukparungsee, R. Sunthornwat, Statistical Design for Monitoring Process Mean on Modified EWMA Control Chart based on Autocorrelated Data. WSEAS Transactions on Computer Research. Vol.11, 2023, pp. 450-464. https://doi.org/10.37394/232018.2023.11.41.

[15] O. J. Osimobi, B. Yorkor, C.A. Nwankwo, Evaluation of daily pollutant standard index and air quality index in a university campus in Nigeria using PM10 and PM2. 5 particulate matter. *Journal of Science, Technology and Environment Informatics*, Vol.7, No.2, 2019. pp. 517-532. https://doi.org/10.18801/jstei.070219.54.

[16] V. Santhana Lakshmi, M. S. Vijaya, A Study on Machine Learning-Based Approaches for PM2.5 Prediction. *In Sustainable Communication Networks and Application: Proceedings of ICSCN 2021*, *Singapore*: *Springer Nature Singapore*, 2022, pp. 163-175. https://doi.org/10.1007/978-981-16-6605-6_11.

[17] R. S. Palais, (2007). A simple proof of the Banach contraction principle, *Journal of Fixed Point Theory and Applications*, Vol 2, 2007, pp. 221-223 , https://doi.org/10.1007/s11784-007-0041-6.

APPENDIX

Table 1. The numerical results of explicit formulas and NIE method with MA(1) process for different choices of θ with $\mu = 2$, k_1=2 and k_2=1.5

	Coefficients of process		Methods	Shift size									
λ	θ_1	f		0.001	0.003	0.005	0.01	0.03	0.05	0.1	0.3	0.5	1.0
0.05	0.10	0.52314389	Explicit	228.710	129.832	90.747	51.926	19.443	12.141	6.477	2.656	1.917	1.400
			CPU_{Exp}	<0.001	<0.001	<0.001	<0.001	<0.001	<0.001	<0.001	<0.001	<0.001	<0.001
			NIE	228.710	129.832	90.747	51.926	19.443	12.141	6.477	2.656	1.917	1.400
			CPU_{NIE}	10.000	11.046	10.141	10.125	10.047	9.703	9.875	10.156	9.516	9.844
			%ACC	100.00	100.00	100.00	100.00	100.00	100.00	100.00	100.00	100.00	100.00
	-0.10	0.639939932	Explicit	234.214	135.235	95.168	54.826	20.646	12.907	6.887	2.810	2.015	1.453
			CPU_{Exp}	<0.001	<0.001	<0.001	<0.001	<0.001	<0.001	<0.001	<0.001	<0.001	<0.001
			NIE	234.214	135.235	95.168	54.826	20.646	12.907	6.887	2.810	2.015	1.453
			CPU_{NIE}	9.922	10.484	10.703	10.516	10.687	10.250	9.938	10.015	10.094	10.109
			%ACC	100.00	100.00	100.00	100.00	100.00	100.00	100.00	100.00	100.00	100.00
	0.20	0.473051522	Explicit	226.025	127.262	88.665	50.573	18.887	11.788	6.288	2.585	1.872	1.376
			CPU_{Exp}	<0.001	<0.001	<0.001	<0.001	<0.001	<0.001	<0.001	<0.001	<0.001	<0.001
			NIE	226.025	127.262	88.665	50.573	18.887	11.788	6.288	2.585	1.872	1.376
			CPU_{NIE}	9.766	11.000	10.985	10.172	10.290	10.110	9.703	9.719	9.532	9.703
			%ACC	100.00	100.00	100.00	100.00	100.00	100.00	100.00	100.00	100.00	100.00
	-0.20	0.707866223	Explicit	237.040	138.081	97.521	56.387	21.299	13.323	7.111	2.895	2.070	1.482
			CPU_{Exp}	<0.001	<0.001	<0.001	<0.001	<0.001	<0.001	<0.001	<0.001	<0.001	<0.001
			NIE	237.040	138.081	97.521	56.387	21.299	13.323	7.111	2.895	2.070	1.482
			CPU_{NIE}	9.891	9.828	9.844	10.094	9.656	10.031	9.797	10.047	9.953	9.938
			%ACC	100.00	100.00	100.00	100.00	100.00	100.00	100.00	100.00	100.00	100.00
	0.30	0.4277822	Explicit	223.380	124.772	86.660	49.279	18.359	11.453	6.110	2.519	1.830	1.354
			CPU_{Exp}	<0.001	<0.001	<0.001	<0.001	<0.001	<0.001	<0.001	<0.001	<0.001	<0.001
			NIE	223.380	124.772	86.660	49.279	18.359	11.453	6.110	2.519	1.830	1.354
			CPU_{NIE}	9.734	9.656	9.735	10.156	9.704	9.718	9.953	9.844	9.954	9.953
			%ACC	100.00	100.00	100.00	100.00	100.00	100.00	100.00	100.00	100.00	100.00
	-0.30	0.78307525	Explicit	239.921	141.035	99.982	58.031	21.991	13.766	7.349	2.985	2.128	1.514
			CPU_{Exp}	<0.001	<0.001	<0.001	<0.001	<0.001	<0.001	<0.001	<0.001	<0.001	<0.001
			NIE	239.921	141.035	99.982	58.031	21.991	13.766	7.349	2.985	2.128	1.514
			CPU_{NIE}	10.609	10.282	10.172	10.672	9.750	9.625	9.781	9.703	9.688	9.657
			%ACC	100.00	100.00	100.00	100.00	100.00	100.00	100.00	100.00	100.00	100.00
0.10	0.10	0.52998795	Explicit	225.925	127.180	88.609	50.553	18.904	11.813	6.318	2.612	1.895	1.391
			CPU_{Exp}	<0.001	<0.001	<0.001	<0.001	<0.001	<0.001	<0.001	<0.001	<0.001	<0.001
			NIE	225.925	127.180	88.609	50.553	18.904	11.813	6.318	2.612	1.895	1.391
			CPU_{NIE}	9.750	9.672	9.890	9.672	10.032	9.796	9.563	9.563	9.500	9.844
			%ACC	100.00	100.00	100.00	100.00	100.00	100.00	100.00	100.00	100.00	100.00
	-0.10	0.649218033	Explicit	231.617	132.674	93.075	53.464	20.103	12.576	6.726	2.765	1.992	1.444
			CPU_{Exp}	<0.001	<0.001	<0.001	<0.001	<0.001	<0.001	<0.001	<0.001	<0.001	<0.001
			NIE	231.617	132.674	93.075	53.464	20.103	12.576	6.726	2.765	1.992	1.444
			CPU_{NIE}	9.734	9.656	9.407	9.657	9.765	9.782	9.719	9.797	9.734	9.781
			%ACC	100.00	100.00	100.00	100.00	100.00	100.00	100.00	100.00	100.00	100.00
	0.20	0.47895424	Explicit	223.158	124.578	86.515	49.202	18.352	11.464	6.132	2.543	1.851	1.368
			CPU_{Exp}	<0.001	<0.001	<0.001	<0.001	<0.001	<0.001	<0.001	<0.001	<0.001	<0.001
			NIE	223.158	124.578	86.515	49.202	18.352	11.464	6.132	2.543	1.851	1.368
			CPU_{NIE}	10.188	9.906	10.140	9.860	10.219	10.265	9.828	9.516	9.484	9.734
			%ACC	100.00	100.00	100.00	100.00	100.00	100.00	100.00	100.00	100.00	100.00
	-0.20	0.718714842	Explicit	234.550	135.582	95.463	55.037	20.758	12.992	6.950	2.850	2.046	1.473
			CPU_{Exp}	<0.001	<0.001	<0.001	<0.001	<0.001	<0.001	<0.001	<0.001	<0.001	<0.001
			NIE	234.550	135.582	95.463	55.037	20.758	12.992	6.950	2.850	2.046	1.473
			CPU_{NIE}	9.859	9.688	9.532	9.750	9.750	9.937	9.828	9.906	9.844	9.734
			%ACC	100.00	100.00	100.00	100.00	100.00	100.00	100.00	100.00	100.00	100.00
	0.30	0.4328869	Explicit	220.441	122.063	84.505	47.913	17.829	11.132	5.956	2.477	1.809	1.346
			CPU_{Exp}	<0.001	<0.001	<0.001	<0.001	<0.001	<0.001	<0.001	<0.001	<0.001	<0.001
			NIE	220.441	122.063	84.505	47.913	17.829	11.132	5.956	2.477	1.809	1.346
			CPU_{NIE}	9.843	9.985	9.969	9.782	9.812	10.016	10.000	9.844	10.047	10.328
			%ACC	100.00	100.00	100.00	100.00	100.00	100.00	100.00	100.00	100.00	100.00
	-0.30	0.795796574	Explicit	237.550	138.611	97.970	56.701	21.455	13.437	7.188	2.940	2.104	1.505
			CPU_{Exp}	<0.001	<0.001	<0.001	<0.001	<0.001	<0.001	<0.001	<0.001	<0.001	<0.001
			NIE	237.550	138.611	97.970	56.701	21.455	13.437	7.188	2.940	2.104	1.505
			CPU_{NIE}	10.079	10.375	10.265	10.250	9.812	9.719	9.875	9.687	9.516	9.672
			%ACC	100.00	100.00	100.00	100.00	100.00	100.00	100.00	100.00	100.00	100.00

Table 2. The numerical results of explicit formulas and NIE method with MA(3) process for different choices of θ_3 with $\mu = 2, \theta_1 = 0.1, \theta_2 = 0.2,$ k_1=3 and k_2=2.5

	Coefficients of process		Methods	Shift size									
λ	θ_3	f		0.001	0.003	0.005	0.01	0.03	0.05	0.1	0.3	0.5	1.0
0.05	0.10	0.62914781	Explicit	209.529	112.418	76.950	43.202	16.032	10.052	5.444	2.346	1.747	1.326
			CPU_{Exp}	<0.001	<0.001	<0.001	<0.001	<0.001	<0.001	<0.001	<0.001	<0.001	<0.001
			NIE	209.529	112.418	76.950	43.202	16.032	10.052	5.444	2.346	1.747	1.326
			CPU_{NIE}	10.000	9.922	10.172	10.016	9.906	10.031	9.984	9.875	9.781	9.735
			%ACC	100.00	100.00	100.00	100.00	100.00	100.00	100.00	100.00	100.00	100.00
	-0.10	0.769378422	Explicit	214.996	117.200	80.694	45.555	16.975	10.649	5.763	2.467	1.824	1.368
			CPU_{Exp}	<0.001	<0.001	<0.001	<0.001	<0.001	<0.001	<0.001	<0.001	<0.001	<0.001
			NIE	214.996	117.200	80.694	45.555	16.975	10.649	5.763	2.467	1.824	1.368
			CPU_{NIE}	9.890	10.095	10.375	9.812	10.078	10.438	10.172	10.703	10.078	10.312
			%ACC	100.00	100.00	100.00	100.00	100.00	100.00	100.00	100.00	100.00	100.00
	0.20	0.568978922	Explicit	206.865	110.144	75.185	42.102	15.594	9.776	5.296	2.291	1.711	1.307
			CPU_{Exp}	<0.001	<0.001	<0.001	<0.001	<0.001	<0.001	<0.001	<0.001	<0.001	<0.001
			NIE	206.865	110.144	75.185	42.102	15.594	9.776	5.296	2.291	1.711	1.307
			CPU_{NIE}	9.625	9.860	9.766	9.703	9.828	9.890	9.906	9.813	10.016	10.000
			%ACC	100.00	100.00	100.00	100.00	100.00	100.00	100.00	100.00	100.00	100.00
	-0.20	0.85089532	Explicit	217.805	119.716	82.681	46.816	17.484	10.971	5.936	2.533	1.867	1.391
			CPU_{Exp}	<0.001	<0.001	<0.001	<0.001	<0.001	<0.001	<0.001	<0.001	<0.001	<0.001
			NIE	217.805	119.716	82.681	46.816	17.484	10.971	5.936	2.533	1.867	1.391
			CPU_{NIE}	9.750	10.140	10.063	9.969	9.969	10.093	10.110	9.812	10.047	10.015
			%ACC	100.00	100.00	100.00	100.00	100.00	100.00	100.00	100.00	100.00	100.00
	0.30	0.51458996	Explicit	204.247	107.941	73.485	41.048	15.177	9.513	5.156	2.238	1.678	1.289
			CPU_{Exp}	<0.001	<0.001	<0.001	<0.001	<0.001	<0.001	<0.001	<0.001	<0.001	<0.001
			NIE	204.247	107.941	73.485	41.048	15.177	9.513	5.156	2.238	1.678	1.289
			CPU_{NIE}	9.500	9.578	9.922	9.641	9.891	9.593	10.000	9.829	9.782	9.968
			%ACC	100.00	100.00	100.00	100.00	100.00	100.00	100.00	100.00	100.00	100.00
	-0.30	0.94111916	Explicit	220.667	122.324	84.755	48.139	18.021	11.313	6.119	2.603	1.913	1.417
			CPU_{Exp}	<0.001	<0.001	<0.001	<0.001	<0.001	<0.001	<0.001	<0.001	<0.001	<0.001
			NIE	220.667	122.324	84.755	48.139	18.021	11.313	6.119	2.603	1.913	1.417
			CPU_{NIE}	9.890	9.907	9.906	9.954	10.250	10.046	10.016	9.875	9.875	9.875
			%ACC	100.00	100.00	100.00	100.00	100.00	100.00	100.00	100.00	100.00	100.00
0.10	0.10	0.634297242	Explicit	207.861	110.997	75.851	42.525	15.774	9.896	5.368	2.325	1.736	1.322
			CPU_{Exp}	<0.001	<0.001	<0.001	<0.001	<0.001	<0.001	<0.001	<0.001	<0.001	<0.001
			NIE	207.861	110.997	75.851	42.525	15.774	9.896	5.368	2.325	1.736	1.322
			CPU_{NIE}	9.500	9.500	9.797	9.812	9.797	10.016	9.719	9.562	9.594	10.015
			%ACC	100.00	100.00	100.00	100.00	100.00	100.00	100.00	100.00	100.00	100.00
	-0.10	0.7765555	Explicit	213.467	115.853	79.640	44.898	16.722	10.495	5.688	2.446	1.813	1.364
			CPU_{Exp}	<0.001	<0.001	<0.001	<0.001	<0.001	<0.001	<0.001	<0.001	<0.001	<0.001
			NIE	213.467	115.853	79.609	44.898	16.722	10.495	5.688	2.446	1.813	1.364
			CPU_{NIE}	9.875	10.063	9.609	9.890	10.015	9.860	9.891	9.781	9.859	10.021
			%ACC	100.00	100.00	100.00	100.00	100.00	100.00	100.00	100.00	100.00	100.00
	0.20	0.573357662	Explicit	205.139	108.695	74.071	41.419	15.336	9.619	5.221	2.270	1.701	1.303
			CPU_{Exp}	<0.001	<0.001	<0.001	<0.001	<0.001	<0.001	<0.001	<0.001	<0.001	<0.001
			NIE	205.139	108.695	74.071	41.419	15.336	9.619	5.221	2.270	1.701	1.303
			CPU_{NIE}	9.828	9.703	9.813	9.937	9.922	10.000	9.750	9.891	9.922	9.766
			%ACC	100.00	100.00	100.00	100.00	100.00	100.00	100.00	100.00	100.00	100.00
	-0.20	0.859400677	Explicit	216.356	118.419	81.660	46.174	17.236	10.820	5.862	2.512	1.856	1.387
			CPU_{Exp}	<0.001	<0.001	<0.001	<0.001	<0.001	<0.001	<0.001	<0.001	<0.001	<0.001
			NIE	216.356	118.419	81.660	46.174	17.236	10.820	5.862	2.512	1.856	1.387
			CPU_{NIE}	10.125	10.109	10.390	10.110	10.296	10.079	10.218	9.875	9.844	9.875
			%ACC	100.00	100.00	100.00	100.00	100.00	100.00	100.00	100.00	100.00	100.00
	0.30	0.518323125	Explicit	202.468	106.471	72.361	40.363	14.919	9.357	5.081	2.218	1.667	1.285
			CPU_{Exp}	<0.001	<0.001	<0.001	<0.001	<0.001	<0.001	<0.001	<0.001	<0.001	<0.001
			NIE	202.468	106.471	72.361	40.363	14.919	9.357	5.081	2.218	1.667	1.285
			CPU_{NIE}	10.047	10.125	10.453	10.250	10.250	10.141	10.266	10.359	10.328	9.797
			%ACC	100.00	100.00	100.00	100.00	100.00	100.00	100.00	100.00	100.00	100.00
	-0.30	0.951223605	Explicit	219.308	121.086	83.773	47.519	17.780	11.165	6.047	2.583	1.902	1.412
			CPU_{Exp}	<0.001	<0.001	<0.001	<0.001	<0.001	<0.001	<0.001	<0.001	<0.001	<0.001
			NIE	219.308	121.086	83.773	47.519	17.780	11.165	6.047	2.583	1.902	1.412
			CPU_{NIE}	9.797	10.000	9.845	10.093	9.907	10.187	9.609	9.484	9.797	9.718
			%ACC	100.00	100.00	100.00	100.00	100.00	100.00	100.00	100.00	100.00	100.00

Table 3. One-sided comparison of the ARL for the MA(2) Process on standard, modified and new modified EWMA control charts with $\mu = 1.5, \theta_1 = 0.1, \theta_2 = 0.2$

λ	Shift size	EWMA	modified EWMA	New modified EWMA (k_1=3)			
			k=3	k_2=2.8	k_2=2.4	k_2=2.0	k_2=1.6
		h= 0.0000000311349	*b*=2.50077903	*f*=1.2192197	*f*=1.1140715	*f*=0.975974687	*f*=0.855121645
0.05	0.000	370.000	370.000	370.000	370.000	370.000	370.000
	0.001	362.267	252.837	229.575	225.585	221.713	217.944
	0.003	347.326	155.027	130.735	126.911	123.288	119.842
	0.005	333.058	111.941	91.534	88.435	85.525	82.781
	0.01	300.120	66.286	52.524	50.508	48.633	46.879
	0.03	199.917	25.675	19.825	18.991	18.223	17.510
	0.05	135.303	16.214	12.460	11.929	11.440	10.988
	0.10	54.470	8.770	6.738	6.451	6.188	5.944
	0.30	3.682	3.632	2.843	2.732	2.630	2.536
	0.50	**1.292**	2.587	2.069	1.996	1.930	1.869
	1.00	**1.007**	1.799	1.504	1.463	1.426	1.393
	RMI	3.7575	0.4417	0.1806	0.1428	0.1079	0.0754
	AEQL	0.2515	0.2668	0.2184	0.2116	0.2055	0.1999
		h=0.001320183	*b*=2.55353675	*f*=1.286970882	*f*=1.12823002	*f*=0.989389065	*f*=0.867879192
0.10	0.000	370.000	370.000	370.000	370.000	370.000	370.000
	0.001	365.860	252.948	228.495	224.415	220.468	216.639
	0.003	357.741	155.152	129.695	125.813	122.147	118.672
	0.005	349.834	112.049	90.693	87.554	84.618	81.860
	0.01	330.947	66.362	51.981	49.945	48.059	46.301
	0.03	266.465	25.709	19.607	18.769	17.999	17.287
	0.05	216.296	16.236	12.328	11.794	11.305	10.853
	0.10	132.687	8.783	6.673	6.385	6.122	5.880
	0.30	27.501	3.638	2.824	2.713	2.612	2.519
	0.50	9.024	2.591	2.059	1.986	1.920	1.860
	1.00	2.092	1.801	1.500	1.459	1.423	1.389
	RMI	7.3918	0.3534	0.0992	0.0634	0.0306	0.0000
	AEQL	0.8160	0.2672	0.2175	0.2108	0.2047	0.1991
		h=0.0546309595	*b*=2.6650348	*f*=1.317963312	*f*=1.15728376	*f* =1.01682627	*f*=0.8938998
0.20	0.000	370.000	370.000	370.000	370.000	370.000	370.000
	0.001	361.885	253.388	226.498	222.243	218.152	214.205
	0.003	346.523	155.648	127.791	123.794	120.047	116.516
	0.005	332.220	112.479	89.155	85.941	82.956	80.169
	0.01	300.446	66.661	50.992	48.918	47.010	45.245
	0.03	212.114	25.840	19.216	18.367	17.593	16.881
	0.05	159.036	16.321	12.088	11.549	11.058	10.607
	0.10	90.111	8.829	6.554	6.265	6.002	5.761
	0.30	22.463	3.656	2.789	2.679	2.578	2.487
	0.50	9.857	2.603	2.040	1.968	1.904	1.845
	1.00	3.278	1.808	1.492	1.452	1.416	1.384
	RMI	5.9447	0.3804	0.1013	0.0646	0.0310	0.0000
	AEQL	0.8450	0.2683	0.2159	0.2092	0.2032	0.1978

Table 4. Two-sided comparison of the ARL for the MA(3) process on standard, modified and new modified EWMA control charts with $\mu = 1, \theta_1 = 0.1, \theta_2 = 0.2$ and $\theta_3 = 0.3$

λ	Shift size	EWMA	modified EWMA	New modified EWMA (k_1=2)			
			k=2	k_2=1.8	k_2=1.4	k_2=1.0	k_2=0.6
		h=0.0050002826177	b=3.91920448	f=1.1073299	f=0.92684295	f=0.77897484	f=0.657739777
0.05	0.000	370.000	370.000	370.000	370.000	370.000	370.000
	0.001	362.947	313.020	243.579	237.608	231.906	226.418
	0.003	349.283	239.335	144.885	138.679	132.967	127.656
	0.005	336.185	193.752	103.233	98.035	93.322	89.000
	0.01	305.754	131.299	60.250	56.756	53.637	50.816
	0.03	211.164	57.488	22.978	21.497	20.193	19.028
	0.05	147.964	36.905	14.424	13.476	12.642	11.901
	0.10	64.553	19.632	7.735	7.222	6.774	6.375
	0.30	5.188	7.212	3.163	2.966	2.794	2.644
	0.50	**1.561**	4.687	2.254	2.126	2.015	1.918
	1.00	**1.020**	2.824	1.591	1.520	1.459	1.406
RMI		3.7956	1.4290	0.2172	0.1566	0.1031	0.0552
AEQL		0.2841	0.4551	0.2349	0.2230	0.2128	0.2039
		h= 0.01756565	b= 4.1197240	f=1.1252408	f=0.94370181	f=0.7948526	f=0.672631283
0.10	0.000	370.000	370.000	370.000	370.000	370.000	370.000
	0.001	366.499	316.102	241.779	235.679	229.883	224.330
	0.003	359.616	244.789	142.997	136.733	130.999	125.693
	0.005	352.887	199.734	101.649	96.429	91.721	87.425
	0.01	336.719	136.802	59.191	55.701	52.601	49.811
	0.03	280.353	60.575	22.545	21.073	19.784	18.637
	0.05	235.005	38.954	14.157	13.216	12.394	11.665
	0.10	155.363	20.694	7.603	7.096	6.654	6.263
	0.30	40.631	7.521	3.125	2.931	2.762	2.615
	0.50	15.341	4.851	2.234	2.108	1.999	1.904
	1.00	3.607	2.892	1.583	1.513	1.453	1.402
RMI		8.3140	1.4335	0.1547	0.0967	0.0456	0.0000
AEQL		1.2308	0.4692	0.2331	0.2215	0.2114	0.2028
		h=0.23758671	b=4.5895106	f=1.16237634	f=0.978406432	f =0.82736342	f=0.703014971
0.20	0.000	370.000	370.000	370.000	370.000	370.000	370.000
	0.001	365.277	323.688	238.514	232.173	226.199	220.522
	0.003	356.109	258.835	139.628	133.256	127.476	122.176
	0.005	347.295	215.590	98.843	93.579	88.877	84.624
	0.01	326.687	151.986	57.327	53.840	50.773	48.036
	0.03	260.559	69.493	21.787	20.331	19.066	17.950
	0.05	212.887	44.932	13.690	12.762	11.958	11.250
	0.10	138.440	23.794	7.372	6.874	6.444	6.066
	0.30	43.146	8.403	3.058	2.869	2.706	2.564
	0.50	20.509	5.311	2.198	2.076	1.971	1.880
	1.00	6.868	3.078	1.569	1.501	1.444	1.394
RMI		8.5819	1.7633	0.1563	0.0973	0.0458	0.0000
AEQL		1.6431	0.5089	0.2301	0.2188	0.2091	0.2007

Table 5. One-sided comparison of the ARL for the MA(1) Process on EWMA, modified and new modified EWMA control charts with $\mu = 36.326$, $\theta_1 = -0.526$

λ	Shift size	EWMA	modified EWMA	New modified EWMA (k_1=3)			
			k=3	k_2=2.8	k_2=2.6	k_2=2.4	k_2=2.0
		h=0.065747402	b=4.3083842	f=4.28970497	f=4.27110692	f=4.2525897	f=4.21579633
0.05	0.000	370.000	370.000	370.000	370.000	370.000	370.000
	0.001	360.943	341.302	341.272	341.243	341.214	341.156
	0.003	344.093	295.488	295.422	295.357	295.291	295.160
	0.005	328.743	260.539	260.455	260.370	260.285	260.116
	0.01	295.744	201.138	201.037	200.937	200.836	200.634
	0.03	210.913	105.418	105.335	105.252	105.170	105.005
	0.05	163.801	71.586	71.523	71.460	71.397	71.271
	0.10	104.932	39.933	39.894	39.855	39.817	39.739
	0.30	42.654	14.818	14.803	14.788	14.773	14.743
	0.50	26.544	9.332	9.323	9.313	9.304	9.285
	1.00	13.448	5.110	5.105	5.100	5.095	5.085
RMI		0.9369	0.0031	0.0025	0.0019	0.0012	0.0000
AEQL		2.3284	0.8618	0.8609	0.8601	0.8592	0.8575
		h=0.132362494	b=4.38465104	f=4.152556432	f=4.17038365	f=4.18828775	f=4.22432794
0.10	0.000	370.000	370.000	370.000	370.000	370.000	370.000
	0.001	353.007	341.335	340.967	340.996	341.025	341.083
	0.003	323.312	295.563	294.737	294.802	294.867	294.997
	0.005	298.228	260.637	259.568	259.652	259.736	259.904
	0.01	249.792	201.254	199.984	200.084	200.183	200.383
	0.03	151.476	105.512	104.474	104.556	104.637	104.800
	0.05	108.741	71.658	70.866	70.928	70.990	71.114
	0.10	63.837	39.977	39.491	39.529	39.567	39.643
	0.30	24.225	14.835	14.645	14.660	14.675	14.704
	0.50	15.050	9.342	9.223	9.232	9.242	9.260
	1.00	7.862	5.115	5.052	5.057	5.062	5.072
RMI		0.3612	0.0078	0.0000	0.0006	0.0012	0.0025
AEQL		1.3534	0.8627	0.8519	0.8528	0.8536	0.8553
		h=0.26624494	b=4.53825881	f=4.31375131	f=4.33177155	f=4.34986775	f=4.38628935
0.20	0.000	370.000	370.000	370.000	370.000	370.000	370.000
	0.001	346.929	341.406	341.057	341.086	341.114	341.172
	0.003	308.472	295.722	294.939	295.003	295.067	295.196
	0.005	277.702	260.843	259.829	259.912	259.995	260.162
	0.01	222.307	201.500	200.294	200.392	200.491	200.689
	0.03	123.796	105.713	104.726	104.807	104.887	105.049
	0.05	85.897	71.812	71.057	71.119	71.180	71.304
	0.10	48.817	40.070	39.608	39.645	39.683	39.759
	0.30	18.213	14.871	14.690	14.705	14.719	14.749
	0.50	11.383	9.364	9.251	9.260	9.269	9.288
	1.00	6.094	5.126	5.066	5.071	5.076	5.085
RMI		0.1399	0.0074	0.0000	0.0006	0.0012	0.0024
AEQL		1.0387	0.8646	0.8544	0.8552	0.8561	0.8577

Table 6. Two-sided comparison of the ARL for the MA(2) Process on EWMA, modified and new modified EWMA control charts with $\mu = 41.884, \theta_1 = -0.592, \theta_2 = -0.228$

λ	Shift size	EWMA	modified EWMA	New modified EWMA (k_1=2)			
			k=2	k_2=1.8	k_2=1.4	k_2=1.0	k_2=0.6
		h=0.16122255	b= 2.79310936	f = 2.7774588	f = 2.74591025	f = 2.7147342	f = 2.68392622
0.05	0.000	370.000	370.000	370.000	370.000	370.000	370.000
	0.001	365.930	343.533	342.598	342.524	342.450	342.376
	0.003	358.050	300.554	298.418	298.250	298.082	297.913
	0.005	350.500	267.152	264.351	264.131	263.911	263.692
	0.01	332.937	209.115	205.709	205.443	205.177	204.912
	0.03	277.245	112.088	109.201	108.978	108.755	108.533
	0.05	237.394	76.713	74.483	74.311	74.139	73.968
	0.10	174.353	43.083	41.706	41.600	41.494	41.388
	0.30	83.617	16.027	15.496	15.454	15.412	15.370
	0.50	54.384	10.072	9.746	9.719	9.693	9.667
	1.00	28.328	5.477	5.314	5.300	5.286	5.272
RMI		1.9673	0.0255	0.0049	0.0033	0.0016	0.0000
AEQL		4.7347	0.9265	0.8979	0.8955	0.8931	0.8908
		h=0.224185655	b=2.86081467	f=2.84510645	f=2.81346463	f=2.78218898	f=2.75127523
0.10	0.000	370.000	370.000	370.000	370.000	370.000	370.000
	0.001	359.661	343.473	342.605	342.532	342.459	342.386
	0.003	340.626	300.418	298.435	298.269	298.103	297.937
	0.005	323.504	266.972	264.373	264.156	263.939	263.723
	0.01	287.386	208.895	205.735	205.473	205.211	204.950
	0.03	198.655	111.900	109.223	109.003	108.783	108.565
	0.05	151.780	76.567	74.500	74.330	74.161	73.992
	0.10	95.448	42.993	41.717	41.612	41.507	41.403
	0.30	38.391	15.992	15.500	15.458	15.417	15.376
	0.50	24.023	10.050	9.748	9.722	9.696	9.671
	1.00	12.429	5.466	5.315	5.302	5.288	5.274
RMI		0.7588	0.0239	0.0048	0.0032	0.0016	0.0000
AEQL		2.1312	0.9246	0.8981	0.8958	0.8935	0.8911
		h=0.350119145	b=2.99703195	f=2.98120498	f=2.94937072	f=2.91789096	f=2.88676168
0.20	0.000	370.000	370.000	370.000	370.000	370.000	370.000
	0.001	352.489	343.370	342.627	342.556	342.486	342.414
	0.003	322.015	300.181	298.485	298.324	298.163	298.001
	0.005	296.397	266.662	264.439	264.228	264.017	263.806
	0.01	247.246	208.515	205.815	205.560	205.305	205.050
	0.03	148.745	111.576	109.291	109.076	108.862	108.649
	0.05	106.449	76.316	74.552	74.387	74.222	74.057
	0.10	62.340	42.838	41.749	41.646	41.544	41.443
	0.30	23.706	15.932	15.512	15.472	15.432	15.392
	0.50	14.791	10.014	9.756	9.730	9.705	9.680
	1.00	7.808	5.448	5.319	5.306	5.293	5.279
RMI		0.2997	0.0210	0.0047	0.0031	0.0016	0.0000
AEQL		1.3362	0.9214	0.8988	0.8965	0.8943	0.8920

Contribution of Individual Authors to the Creation of a Scientific Article (Ghostwriting Policy)

- Sittikorn Khamrod carried out the writing-original draft preparation and simulation.
- Yupaporn Areepong the concept and conducted validation.
- Saowanit Sukparungsee has implemented the methodology and software.
- Rapin Sunthornwat was responsible for Mathematics and statistics.

Sources of Funding for Research Presented in a Scientific Article or Scientific Article Itself
This research was funded by Thailand Science Research and Innovation Fund (NSRF), and King Mongkut's University of Technology North Bangkok with Contract no. KMUTNB-FF-67-B-12.

Conflicts of Interest
The authors declare no conflict of interest.